JP Journal of Heat and Mass Transfer

http://www.pphmj.com
http://dx.doi.org/10.17654/0973576323013
Volume 32, 2023, Pages 31-46 **P-ISSN: 0973-5763**

MATHEMATICAL ANALYSIS OF MICROPOLAR FLUID IN DARCIAN REGIME FOR THE IMPACT OF HYDROMAGNETIC DRAG FORCE AND DIFFUSION-THERMO: AN ANALYTICAL APPROACH

Mayzul Alom Hussain and Sahin Ahmed*

Department of Mathematics
Rajiv Gandhi University
Rono Hills, Doimukh, Arunachal Pradesh
Pin - 791112, India
e-mail: mayzuljun89@gmail.com
sahin.ahmed@rgu.ac.in

Abstract

The purpose of the present research is to determine how the convective temperature and mass flow affect the hydromagnetic micropolar fluid across a vertical flat surface in a Darcian porous medium. Through the use of boundary conditions and the assumption

Received: August 18, 2022; Accepted: December 26, 2022
Keywords and phrases: hydromagnetic, temperature and mass flow, micropolar fluid, porous media, microrotation.
*Corresponding author

How to cite this article: Mayzul Alom Hussain and Sahin Ahmed, Mathematical analysis of micropolar fluid in Darcian regime for the impact of hydromagnetic drag force and diffusion-thermo: an analytical approach, JP Journal of Heat and Mass Transfer 32 (2023), 31-46.
http://dx.doi.org/10.17654/0973576323013

Published Online: March 20, 2023

of a convergent series, the non-dimensional system of equations is analytically solved, providing the precise values for velocity, microrotation, temperature, and concentration. The novelty of the current study is that it takes heat transfer into account while accounting for the impacts of chemical reaction in a micropolar fluid flow of reactive diffusing species. Visual representations of the impacts of several parameters on temperature, concentration, microrotation, and velocity have been provided in the form of graphs. The rotating fluid's velocity drops but its angular motion increases with increase in M, K_p, Pr, and Gr. This research has wide-ranging applicability in technology and engineering, including thermal conductivity, biological applications, water filtration, aerodynamics, textiles, etc.

Nomenclature

u = velocity in x-direction, ms^{-1}

v = velocity in y-direction, ms^{-1}

N = angular velocity, s^{-1}

C = species concentration, mol/m^3

C_p = specific heat capacity, $J \cdot kg^{-1} \cdot K^{-1}$

D_m = diffusivity of mass, m^2/s

k_r = chemical reaction coefficient, $M.s^{-1}$

k_T = thermal diffusion ratio, m^2/s

B_0 = magnetic induction, Tesla

C_s = coefficient of couple stress, Pa

k = permeability of porous medium, m^2

g = gravitational acceleration, m/s^2

j = microinertia per unit mass, $Kg.m^2$

ν = kinematic viscosity, m^2s^{-1}

α = vortex viscosity, ms^{-1}

ρ = fluid density, kgm^{-3}

μ = dynamic viscosity, Pa.s or $kg.m^{-1}s^{-1}$

k_1 = thermal conductivity, $W{\cdot}m^{-1}K^{-1}$

β_T = coefficient of thermal expansion, K^{-1}

β_C = coefficient of concentration expansion, K^{-1}

σ = electrical conductivity, $S.m^{-1}$

ϕ_1 = porosity of the porous medium, m^2

β = micropolar fluid parameter

Gr = thermal Grashof number

Gm = Grashof number for mass transmission

K_p = porosity

M = magnetic drag force

Pr = Prandtl number

R_a = radiation parameter

Sc = Schmidt number

η = spin gradient

C_r = chemical reaction parameter

Du = Dufour number

1. Introduction

MHD is the study of the interactions between electromagnetic events and conducting fluids. Fluids with microstructures are called *micropolar fluids*. The micropolar fluid theory, put out by Eringen [1, 2], comprises of two separate effects, such as micro-rotational and micro-inertia. The theory of micro structured fluids was studied by Ariman et al. [3, 4]. By looking at velocity, rotational motion, shear, and coupling stress, Ahmadi [5] found that self-similar solutions might appear in the free convection flow of a micropolar fluid across a semi-infinite flat surface when the micro-inertia is not consistent. The micropolar fluid in a boundary layer moving over a flat surface was studied by Peddieson, Jr. [6], who found that the model can forecast outcomes with some of the same characteristics as turbulent boundary shearing layers. Many flow configurations, including vertical plate/channel, stretched sheet, solid sphere, and spinning cone, have been used in research examining the impact of convective transmission of heat of a micropolar fluid/nanofluid/Casson fluid under the application of magnetic drag force in a porous material [7-12]. Bakr [13] published papers on the transmission of heat by convection for micropolar fluids near a rotating sliding vertical surface with thermal radiation and chemical interaction. In the presence of generation/absorption of heat and molar reaction, Chamkha [14] studied the MHD boundary layer flow of fluid motion over a stretched vertical porous surface with uniform motion. In a porous medium with uniform permeability, Vafai and Tien [15] investigated the impact of a fluid inertia force and viscous resistance at boundary in flow and heat transmission. Abo-Eldahab and El Gendy explored convective heat transport along a porous stretched sheet immersed in a non-Darcian permeable medium in the presence of the external magnetic field [16].

The aforementioned investigations provided the inspiration for the current work, where the influence of radiation and heat transfer in porous material, magnetohydrodynamic movement of micropolar fluid over a vertical surface filled with the material of pores has been introduced. The impacts of diffusion-thermo, free convection forces and porosity of the

porous materials over the fluid velocity, angular momentum and temperature have been investigated via MATLAB codes. The analytical solutions are obtained by adopting the classical convergent scheme of infinite series solution.

2. Mathematical Formulation

The recent effort takes into account the two-dimensional, erratic flow of an incompressible, electrically conducting micropolar fluid in a material of pores. The fluid and infinite vertical plate have constant temperature and concentration at rest, which are T_∞ and C_∞, respectively. The temperature and concentration of the plate rise with time to T_ω and C_ω, respectively. The *x*-axis represents the direction of fluid flow down the plate, while the normal to the plate is represented by *y*-axis. The plate is subjected to a consistent magnetic field B_0 in the normal direction. A visual illustration of the situation is presented in Figure 1.

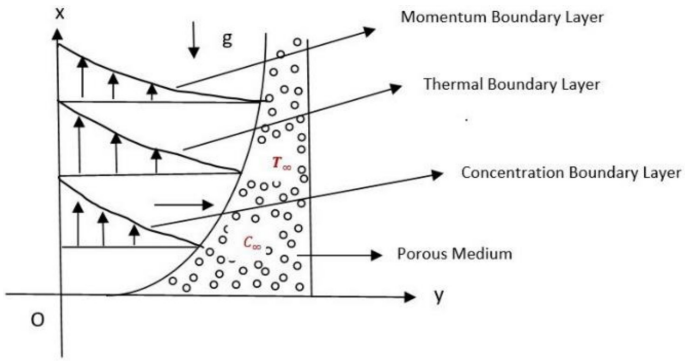

Figure 1. Geometry of the problem.

The present work is an extension of the work done by Sheikh et al. [17].

The governing equations of the micropolar fluid over an oscillating vertical surface with thermophoretic forces are given as follows:

$$\frac{\partial u}{\partial x} + \frac{\partial u}{\partial y} = 0 \Rightarrow \frac{\partial u}{\partial y} = 0, \tag{1}$$

$$\rho\frac{\partial u}{\partial t^*} = \left\{\begin{matrix}(\mu+\alpha)\dfrac{\partial^2 u}{\partial y^2} + \alpha\dfrac{\partial N}{\partial y} - \sigma B_0^2 u - \dfrac{\phi_1\mu}{k}u \\ + \rho g\beta_T(T-T_\infty) + \rho g\beta_C(C-C_\infty)\end{matrix}\right\}, \tag{2}$$

$$\frac{\partial N}{\partial t^*} + u\frac{\partial N}{\partial y} = \frac{\gamma}{\rho j}\frac{\partial^2 N}{\partial y^2}, \tag{3}$$

$$\rho C_p\frac{\partial T}{\partial t^*} = k_1\frac{\partial^2 T}{\partial y^2} - \frac{\partial q_r}{\partial y} + \frac{D_m K_T}{C_s}\frac{\partial^2 C}{\partial y^2}, \tag{4}$$

$$\frac{\partial C}{\partial t^*} = D_m\frac{\partial^2 C}{\partial y^2} - k_r(C-C_\infty). \tag{5}$$

The radioactive heat influx is given by

$$\frac{\partial q_r}{\partial y} = -4a^2(T-T_\infty), \tag{6}$$

where $k > 0$ and $0 < \phi_1 < 1$ and all the notations involved in equations (1) to (6) are described in nomenclature.

Given are the relevant initial and boundary conditions:

$$(u = 0,\ N = 0,\ T = T_\infty,\ C = C_\infty),\ \forall y \ \text{ for } t^* \le 0, \tag{7}$$

$$\left\{\begin{matrix} y = 0 : \left(u = u_0,\ N = -n\dfrac{\partial u}{\partial y},\ T = T_\omega,\ C = C_\omega\right) \\ y \to \infty : (u \to 0,\ N \to 0,\ T \to T_\infty,\ C \to C_\infty)\end{matrix}\right\} \text{ for } t^* > 0. \tag{8}$$

Now, we introduce the dimensionless variables:

$$\left\{v = \frac{u}{u_0},\ \zeta = \frac{u_0}{\nu}y,\ t = \frac{u_0^2}{\nu}t^*,\ \Omega = \frac{\nu N}{u_0^2},\ \theta = \frac{T-T_\infty}{T_\omega - T_\infty},\ \phi = \frac{C-C_\infty}{C_\omega - C_\infty}\right\}. \tag{9}$$

With the help of the dimensionless variables given in equation (9), we transform equations (2)-(5) as follows:

$$\frac{\partial v}{\partial t} = (1+\beta)\frac{\partial^2 v}{\partial \zeta^2} + \beta\frac{\partial \Omega}{\partial \zeta} - k_p v - Mv + Gr\theta + Gm\phi, \tag{10}$$

$$\frac{\partial \Omega}{\partial t} - \frac{\partial \Omega}{\partial \zeta} = \frac{1}{\eta}\frac{\partial^2 \Omega}{\partial \zeta^2}, \tag{11}$$

$$\frac{\partial \theta}{\partial t} = \frac{1}{Pr}\frac{\partial^2 \theta}{\partial \zeta^2} + R_a\theta + Du\frac{\partial^2 \phi}{\partial \zeta^2}, \tag{12}$$

$$\frac{\partial \phi}{\partial t} = \frac{1}{Sc}\frac{\partial^2 \phi}{\partial \zeta^2} - C_r\phi. \tag{13}$$

The following are the transformed initial and boundary conditions:

$$t \le 0: \{V(\zeta, 0) = 0,\ \Omega(\zeta, 0) = 0,\ \theta(\zeta, 0) = 0,\ \phi(\zeta, 0) = 0\},$$

$$t > 0: \begin{Bmatrix} V(0, t) = 1,\ \Omega(0, t) = -n\dfrac{\partial v(0, t)}{\partial \zeta},\ \theta(0, t) = 1,\ \phi(0, t) = 1, \\ v(\infty, t) = 0,\ \Omega(\infty, t) = 0,\ \theta(\infty, t) = 0,\ \phi(\infty, t) = 0 \end{Bmatrix}$$

with physical variables:

$$\begin{Bmatrix} \beta = \dfrac{\alpha}{\mu},\ Gr = \dfrac{\nu g\beta_T}{(T_\omega - T_\infty)u_0^3},\ Gm = \dfrac{\nu g\beta_C}{(C_\omega - C_\infty)u_0^3},\ K_p = \dfrac{ku_0^2}{\nu^2\phi_1}, \\ M = \dfrac{\nu\sigma B_0^2}{\rho u_0^2},\ \eta = \dfrac{\mu j}{\gamma},\ Pr = \dfrac{\mu C_p}{k_1},\ R_a = \dfrac{4a^2}{\rho C_p u_0},\ Sc = \dfrac{\nu}{D_m}, \\ C_r = \dfrac{K_r}{u_0},\ Du = \dfrac{D_m K_T(C_\omega - C_\infty)}{C_s\mu C_p(T_\omega - T_\infty)} \end{Bmatrix}.$$

3. Solution of the Given Problem

Equations (10) to (13) are solved by assuming a series solution:

$$(\zeta, t) = f_0(\zeta) + \varepsilon e^{i\omega t} f_1(\zeta) + o(\varepsilon^2), \tag{14}$$

where $f \equiv v, \Omega, \theta$ or ϕ, $\varepsilon \ll 1$.

Using equation (14) into transformed governing equations (10)-(13) with the help of corresponding transformed boundary conditions, we get the required solutions as

$$\phi = e^{-\sqrt{C_r.Sc}\zeta}; \theta = Ae^{-\sqrt{R_a.Pr}\, i\zeta} + Be^{-\sqrt{C_r.Sc}\zeta}, \tag{15}$$

$$\Omega = Ce^{-\eta\zeta}; v = De^{-E\zeta} + Fe^{-\eta\zeta} + Ge^{-\sqrt{R_a.Pr}\, i\zeta} - He^{-\sqrt{C_r.Sc}\zeta}. \tag{16}$$

4. Results and Discussions

The findings of this investigation have been offered for a number of variables, including the magnetic parameter (M), chemical reaction parameter (C_r), Schmidt number (Sc), Dufour number (Du), permeability parameter (K_p), Prandtl number (Pr), mass Grashof number (Gm), and thermal Grashof number (Gr).

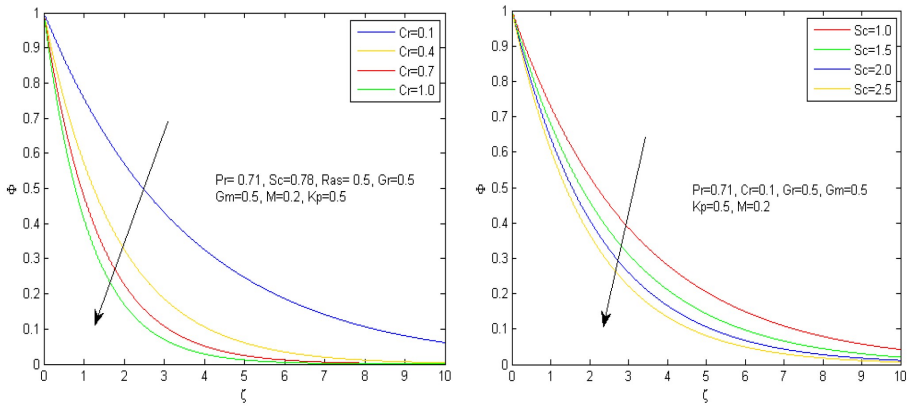

Figure 2. Concentration profiles of C_r and Sc.

Figure 2 illustrates how the Schmidt number (Sc) and chemical reaction parameter (C_r) affect concentration profiles. When C_r is positive, the chemical reaction is endothermic. The higher rate of endothermic chemical reaction leads to a drop in the molar concentration in the rotating fluid, as the endothermic chemical reaction always acts as a mass transfer from the source of the system to the environment of the surface of the molar substance. The Schmidt number can be expressed physically as the product of the momentum diffusivity and the molecular diffusivity coefficient (Sc). The kinematic viscosity predominates over the molecular diffusivity in this figure because all of the Schmidt numbers are larger than or equal to 1 $(Sc \geq 1)$. The higher Schmidt number always thickened the molar concentration boundary layer.

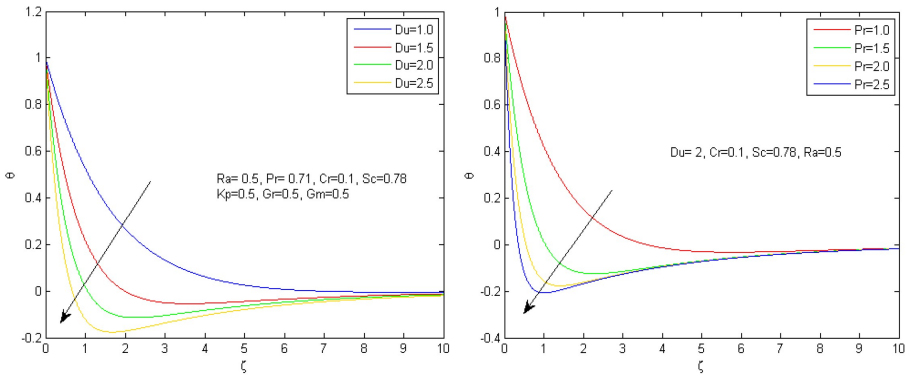

Figure 3. Temperature profiles of *Du* and *Pr*.

In fluid mechanics, the Dufour number (Du) designates the thermal energy flask's input of concentration gradients during flow motion. Temperature depression has happened as a result of the Dufour's effect, since in Figure 3 the concentration gradients dominate the thermal energy in the flow's motion. The figure also displays the fluctuation in the micropolar fluid's temperature field in relation to various Prandtl number values (Pr). The *Prandtl number* is defined as the kinematic diffusivity/thermal

diffusivity ratio for momentum diffusivity (heat diffusivity). A fluid therefore has a lower thermal diffusivity when its Prandtl number is large. Here, when *Pr* rises, the temperature profiles fall. As the Prandtl number increases, the thickness of the thermal boundary layer shrinks.

Figure 4 shows the dual solution of the velocity and microrotation profiles for porosity parameter (K_p) and buoyancy force due to mass transfer. The porosity always serves as a drag force that slows down the movement of the fluid's particles. As a result, the momentum of boundary layer thickens significantly and the motion's acceleration gradually decelerates. The buoyancy force is due to differences which boost the fluid velocity as the viscosity effect is very smaller and thereby molecules are moving freely in the upward direction. Thus, higher values of the permeability parameter produced very porous media, which caused the fluid flow to slow down and cause a decrease in velocity. This graph showed how the permeability parameter (K_p) affected the micro-gyration vector-related microrotation profiles. The relationship between the permeability factor and fluid viscosity is inverse; as the permeability parameter rises, the viscosity falls and the radial velocity rises. As a result, with higher values of K_p, the amplitude of microrotation exhibits a rising behaviour.

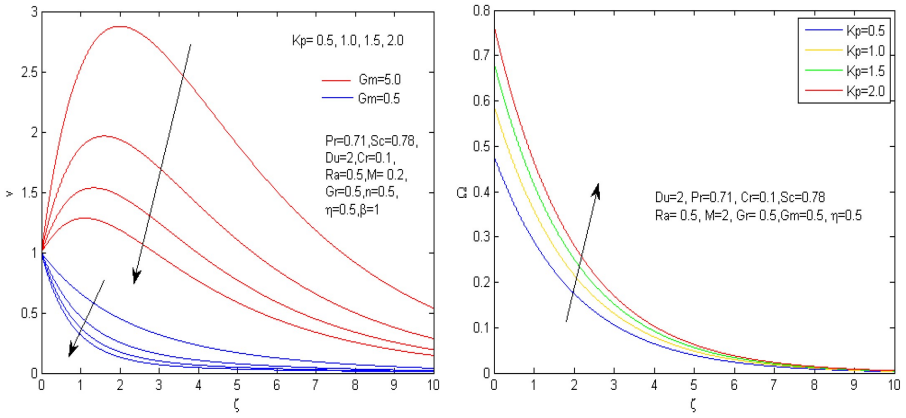

Figure 4. Velocity and microrotation profiles of K_p.

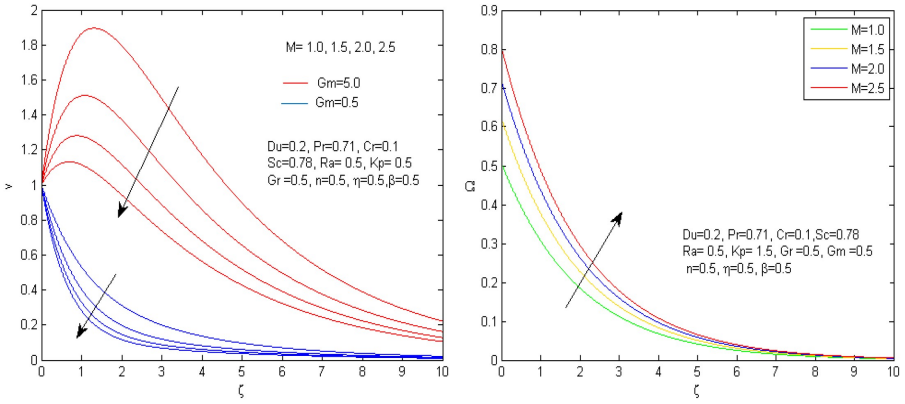

Figure 5. Velocity and microrotation profiles of M.

The dual solution of the velocity distribution and microrotation for magnetic drag force (M) and buoyancy force due to mass transfer has been presented in Figure 5. The magnetic drag force has a retarding effect due to Lorentz force and thereby the molecules of the micropolar fluid are moving with slow motion. Hence, the flow velocity is decelerated by the impact of M and thereby momentum boundary layer thickness reduces as the viscosity effect is pre-dominant near the surface. The buoyancy force is due to differences which boost the fluid velocity as the viscosity effect is very smaller and thereby molecules are moving freely in the upward direction. The figure also showed how magnetic drag force affected the profiles of microrotations. The magnitude of microrotation displays a growing behaviour when the magnitude of the magnetic parameter (M) is raised.

The ratio of kinematic viscosity to thermal diffusivity is referred to as the Prandtl number (Pr) in the context of physics. Considering that the Prandtl number is below or equal to 1 $(Pr \leq 1)$, the kinematic viscosity is lower than thermal diffusivity. Lower Prandtl number means lower kinematic viscosity. In porous media, fluid velocity is inversely proportional to kinematic viscosity. Therefore, in Figure 6, we can see that there is a decline in fluid velocity caused by an increase in kinematic viscosity from top to bottom as the Prandtl number rises from lower values to

higher values. Additionally, this graphic showed how Prandtl number (Pr) affects microrotation profiles. For higher values of Pr, the magnitude of microrotation exhibits a rising behaviour.

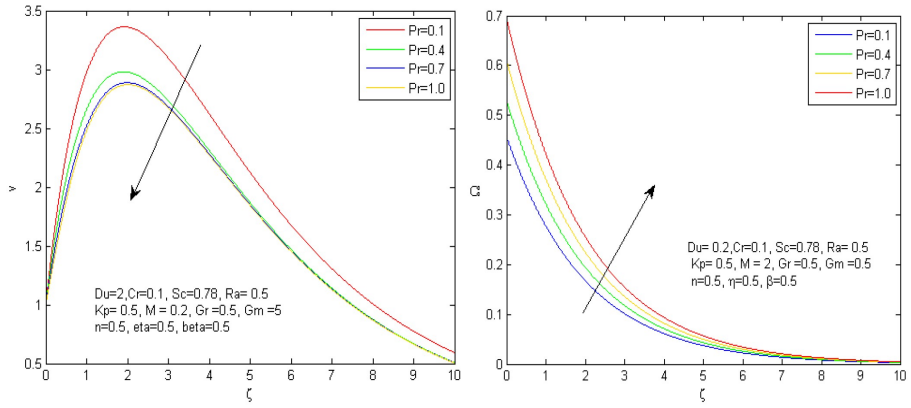

Figure 6. Velocity and microrotation profiles of Pr.

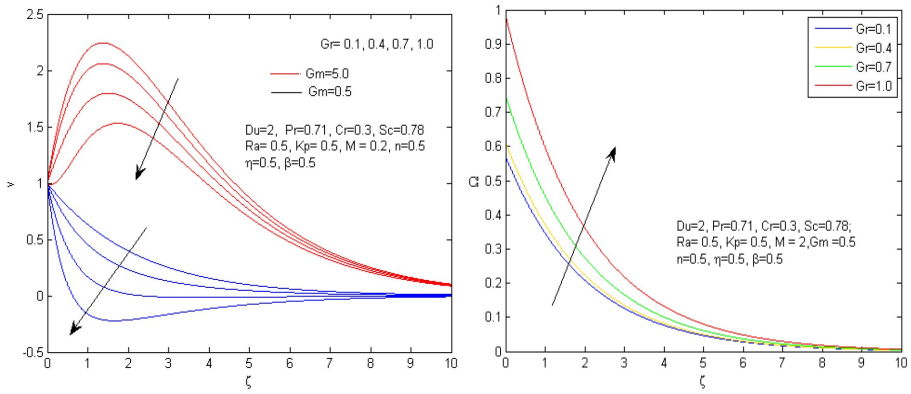

Figure 7. Velocity profiles of thermal Grashof number.

Figure 7 shows how the thermal Grashof number (Gr) affects velocity and microrotation. The graph demonstrates that the thermal Grashof number has a leading influence on accelerating velocities, i.e., a rise in the thermal Grashof number causes a decline in the fluid's motion's velocity. The impact of thermal Grashof number (Gr) on the profiles of microrotations is also

shown in this figure. For higher levels of *Gr*, the magnitude of microrotation exhibits a rising behaviour.

5. Conclusion

The movement of molecules of a micropolar fluid across a vertical surface coated in a Darcian porous material when heated is investigated in this work. To find the precise answers for the present project, the analytical approach is used. Discussion has been done on how different parameters affect temperature, concentration, microrotation, and velocity. The main results from the recent investigation are as follows:

- With increase in permeability parameter (K_p), magnetic parameter (M), Prandtl number (Pr), thermal Grashof number (Gr), declination in fluid velocity has been found.
- In the instance of microrotation, it has been observed that the magnitude of the microrotation profiles decreases with increase in the permeability parameter (K_p), magnetic parameter (M), Prandtl number (Pr), and thermal Grashof number (Gr).
- With increase in Dufour number (Du) and Prandtl number (Pr), fall in temperature has been observed.
- Concentration profiles decline for rise in level of rate of molar reaction (C_r) and Schmidt number (Sc).
- The current work has significant implications for MHD generators and geothermal resource extraction.

Appendices

$$A = 1 + \frac{(DuPr)(C_r Sc)}{C_r Sc + RaPr}; \quad B = -\frac{(DuPr)(C_r Sc)}{C_r Sc + RaPr};$$

$$C = \frac{n}{1 + n\sqrt{\frac{K_p + M}{1+\beta}}\,\frac{\beta\eta}{(1+\beta)\eta^2 - (K_p + M)} - n\eta\,\frac{\beta\eta}{(1+\beta)\eta^2 - (K_p + M)}}$$

$$\times \left[\begin{array}{l} \sqrt{\frac{K_p + M}{1+\beta}}\left(1 - \frac{Gr\left(1 + \frac{(DuPr)(C_rSc)}{C_rSc + R_aPr}\right)}{(1+\beta)(R_aPr) + (K_p + M)}\right. \\ \left. + \frac{Gm - Gr\,\frac{(DuPr)(C_rSc)}{C_rSc + R_aPr}}{(1+\beta)(C_rSc) - (K_p + M)}\right) \\ + \frac{Gr\left(1 + \frac{(DuPr)(C_rSc)}{C_rSc + R_aPr}\right)}{(1+\beta)(R_aPr) + (K_p + M)}\sqrt{R_aPr}\,i \\ - \frac{Gm - Gr\left(\frac{(DuPr)(C_rSc)}{C_rSc + R_aPr}\right)}{(1+\beta)(C_rSc) - (K_p + M)}\sqrt{C_rSc} \end{array}\right];$$

$$D = \left\{\begin{array}{l} 1 - C\,\frac{\beta\eta}{(1+\beta)\eta^2 - (K_p + M)} - \frac{Gr\left(1 + \frac{(DuPr)(C_rSc)}{C_rSc + R_aPr}\right)}{(1+\beta)\cdot(R_a \cdot Pr) + (K_p + M)} \\ + \frac{Gm - Gr\left(\frac{(DuPr)(C_rSc)}{C_rSc + R_aPr}\right)}{(1+\beta)(C_rSc) - (K_p + M)} \end{array}\right\};$$

$$E = \sqrt{\frac{K_p + M}{1+\beta}}; \quad F = C \cdot \frac{\beta\eta}{(1+\beta)\eta^2 - (K_p + M)};$$

$$G = \frac{Gr\left(1 + \frac{(DuPr)(C_rSc)}{C_rSc + R_aPr}\right)}{(1+\beta)(R_aPr) + (K_p + M)}; \quad H = \frac{Gm - Gr\left(\frac{(DuPr)(C_rSc)}{C_rSc + R_aPr}\right)}{(1+\beta)(C_rSc) - (K_p + M)}.$$

References

[1] A. C. Eringen, Simple micro fluids, Int. J. Engng. Sci. 2 (1964), 205-214.

[2] A. C. Eringen, Theory of micropolar fluids, J. Math. Mech. 16 (1966), 1-18.

[3] T. Ariman, M. A. Turk and N. D. Sylvester, Microcontinuum fluid mechanics - a review, Int. J. Engng. Sci. 11 (1973), 905-930.

[4] T. Ariman, M. A. Turk and N. D. Sylvester, Applications of microcontinuum fluid mechanics, Int. J. Engng. Sci. 12 (1974), 273-293.

[5] G. Ahmadi, Self-similar solution of incompressible micropolar boundary layer flow over a semi-infinite plate, Int. J. Engng. Sci. 14 (1976), 639-646.

[6] J. Peddieson, Jr., An application of the micropolar fluid model to the calculation of a turbulent shear flow, Int. J. Engng. Sci. 10 (1972), 23-32.

[7] Y. J. Kim, Heat and mass transfer in MHD micropolar flow over a vertical moving porous plate in a porous medium, Transport in Porous Media 56 (2004), 17-37.

[8] C. S. K. Raju and N. Sandeep, Heat and mass transfer in MHD non-Newtonian bio-convection flow over a rotating cone/plate with cross diffusion, Journal of Molecular Liquids 215 (2016), 115-126.

[9] D. Pal and S. Chatterjee, Heat and mass transfer in MHD non-Darcian flow of a micropolar fluid over a stretching sheet embedded in a porous media with non-uniform heat source and thermal radiation, Commun. Nonlinear Sci. Numer. Simul. 15 (2010), 1843-1857.

[10] S. Hazarika and S. Ahmed, Steady magnetohydrodynamic micropolar Casson fluid of Brownian motion over a solid sphere with thermophoretic and buoyancy forces: numerical analysis, Journal of Nanofluids 9 (2020), 336-345.

[11] S. Hazarika and S. Ahmed, Study of carbon nanotubes with Casson fluid in a vertical channel of porous media for hydromagnetic drag force and diffusion-thermo, J. Sci. Res. 13 (2021), 111-113.

[12] S. Hazarika, S. Ahmed and A. J. Chamkha, Investigation of nanoparticles Cu, Ag and Fe_3O_4 on thermophoresis and viscous dissipation of MHD nanofluid over a stretching sheet in a porous regime: a numerical modelling, Mathematics and Computers in Simulation 182 (2021), 819-837.

[13] A. A. Bakr, Effects of chemical reaction on MHD free convection and mass transfer flow of a micropolar fluid with oscillatory plate velocity and constant heat source in a rotating frame of reference, Commun. Nonlinear Sci. Numer. Simul. 16 (2011), 698-710.

[14] A. J. Chamkha, MHD flow of uniformly stretched vertical permeable surface in the presence of heat generation/absorption and a chemical reaction, Int. Comm. Heat Mass Transfer 30 (2003), 413-422.

[15] K. Vafai and C. L. Tien, Boundary and inertia effects on flow and heat transfer in porous media, Int. J. Heat Transfer 24 (1981), 195-203.

[16] E. M. Abo-Eldahab and M. S. El Gendy, Convective heat transfer past a continuously moving plate embedded in a non-Darcian porous medium in the presence of a magnetic field, Can. J. Phys. 79 (2001), 1031-1038.

[17] N. A. Sheikh, F. Ali, I. Khan, M. Saqib and A. Khan, MHD flow of micropolar fluid over an oscillating vertical plate embedded in porous media with constant temperature and concentration, Mathematical Problems in Engineering (2017), Article ID: 9402964, 1-20. https://doi.org/10.1155/2017/9402964.